Martina Michalikova, Michiel W.H. Remme, Dietmar Schmitz, Susanne Schreiber and Richard Kempter*

Spikelets in pyramidal neurons: generating mechanisms, distinguishing properties, and functional implications

https://doi.org/10.1515/revneuro-2019-0044
Received April 8, 2019; accepted May 13, 2019; previously published online August 22, 2019

Abstract: Spikelets are small spike-like depolarizations that are found in somatic recordings of many neuron types. Spikelets have been assigned important functions, ranging from neuronal synchronization to the regulation of synaptic plasticity, which are specific to the particular mechanism of spikelet generation. As spikelets reflect spiking activity in neuronal compartments that are electrotonically distinct from the soma, four modes of spikelet generation can be envisaged: (1) dendritic spikes or (2) axonal action potentials occurring in a single cell as well as action potentials transmitted via (3) gap junctions or (4) ephaptic coupling in pairs of neurons. In one of the best studied neuron type, cortical pyramidal neurons, the origins and functions of spikelets are still unresolved; all four potential mechanisms have been proposed, but the experimental evidence remains ambiguous. Here we attempt to reconcile the scattered experimental findings in a coherent theoretical framework. We review in detail the various mechanisms that can give rise to spikelets. For each mechanism, we present the biophysical underpinnings as well as the resulting properties of spikelets and compare these predictions to experimental data from pyramidal neurons. We also discuss the functional implications of each mechanism. On the example of pyramidal neurons, we illustrate that several independent spikelet-generating mechanisms fulfilling vastly different functions might be operating in a single cell.

Keywords: action potential initiation; axon initial segment; dendritic spikes; ephaptic coupling; gap junction.

***Corresponding author: Richard Kempter,** Institute for Theoretical Biology, Department of Biology, Humboldt-Universität zu Berlin, D-10115 Berlin, Germany; Bernstein Center for Computational Neuroscience Berlin, Philippstr. 13, D-10115 Berlin, Germany; and Einstein Center for Neurosciences Berlin, D-10117 Berlin, Germany, e-mail: r.kempter@biologie.hu-berlin.de
Martina Michalikova and Michiel W.H. Remme: Institute for Theoretical Biology, Department of Biology, Humboldt-Universität zu Berlin, D-10115 Berlin, Germany
Dietmar Schmitz: Neuroscience Research Center, Charite-University Medicine, D-10117 Berlin, Germany; Bernstein Center for Computational Neuroscience Berlin, D-10115 Berlin, Germany; Einstein Center for Neurosciences Berlin, D-10117 Berlin, Germany; Berlin Institute of Health, D-10178 Berlin, Germany; Cluster of Excellence NeuroCure, D-10117 Berlin, Germany; German Center for Neurodegenerative Diseases (DZNE) Berlin, D-10117 Berlin, Germany; and Max-Delbrück-Centrum für Molekulare Medizin, Berlin, Germany
Susanne Schreiber: Institute for Theoretical Biology, Department of Biology, Humboldt-Universität zu Berlin, D-10115 Berlin, Germany; Bernstein Center for Computational Neuroscience Berlin, Philippstr. 13, D-10115 Berlin, Germany; and Einstein Center for Neurosciences Berlin, D-10117 Berlin, Germany

Introduction

Spikelets are non-synaptic events of small amplitudes (<30 mV) that are observed in intracellular recordings of many types of neurons (e.g. in thalamocortical neurons, Hughes et al., 2002; thalamic reticular neurons, Fuentealba et al., 2004; hippocampal interneurons, Zhang et al., 2004). Because of their spike-like appearance and all-or-none character, spikelets are considered to originate in action potentials (APs) generated in electrotonically distinct neuronal compartments, when currents from a remote AP influence the membrane voltage of the recorded compartment but do not suffice to initiate an AP there. As spikelets are typically measured in somatic recordings, the underlying APs might, in principle, occur in dendritic or axonal compartments within the same cell or in another cell coupled by gap junctions or ephaptically through extracellular fields (Figure 1).

As each of these mechanisms has different functional implications, it is important to determine the origin of spikelets to assess their potential computational role in a given system.

One factor that complicates (comparative) spikelet studies and contributes to the confusion about their origin is the many different names for spikelets that can be found in the literature. These alternative names, sometimes reflecting the presumed origin of spikelets, include the following: 'IS spikes' (IS: initial segment; Coombs et al., 1957), 'fast

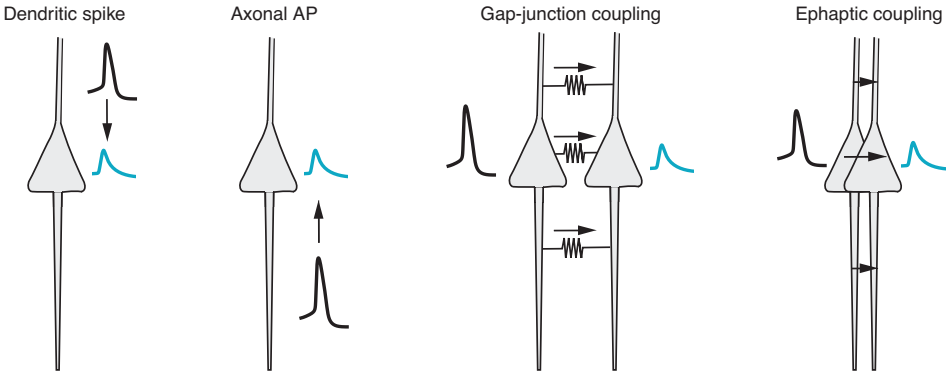

Figure 1: Mechanisms of spikelet generation.
Somatic spikelets (blue traces) can result from propagation failures of dendritic spikes or axonal APs as well as from AP transmission through gap junctions or ephaptic transmission through extracellular fields.

prepotentials' (FPPs; Spencer and Kandel, 1961), 'short-latency depolarizations' (Llinas et al., 1974), 'd-spikes' (d: dendritic; Wong and Stewart, 1992), 'partial spikes' (Zhang et al., 1998), 'small spikes' (Connors and Kriegstein, 1986), 'third potentials' (Kaplan and Shapley, 1984), and 'ePSPs' (electrical PSPs; Gibson et al., 2005).

The question of spikelet origin is resolved for some systems. For example, spikelets in cortical interneurons were found to result from electrotonic coupling by dendrodendritic and somatodendritic gap junctions, which increases the firing synchrony of interneurons and promotes generation and maintenance of network oscillations (Bennett and Zukin, 2004). In contrast, the origin of spikelets in cortical pyramidal neurons is still not settled. Virtually all possible spikelet mechanisms have been hypothesized to explain spikelet occurrence in these cells, but the experimental evidence is ambiguous.

In this article, we focus on spikelets in cortical pyramidal neurons. We first describe the properties of spikelets, noting that there are at least two qualitatively distinct spikelet types occurring in these cells. Then, we review the various mechanisms that can give rise to spikelets. We present theoretical considerations about spikelet properties generated by each of the possible mechanisms and compare them to experimental data from pyramidal neurons. We also discuss the functional implications of each type of spikelet.

Properties of spikelets in pyramidal neurons

At least two qualitatively different spikelet types have been observed in cortical pyramidal cells (Figure 2). The first spikelet type (Figure 2A, B) is characterized by relatively large amplitudes (typically in the range of 10 mV) and fast rise dynamics (max. dV/dt of 10–40 V/s). The decay is often, but not always, biphasic, with an initial faster phase (time constant <1 ms) followed by a slower phase (time constant >5 ms; Figure 2A, B right). These large-amplitude spikelets show an all-or-none behavior, and in a single cell there is usually one, rarely two, discrete amplitudes of spikelets (Schmitz et al., 2001; Crochet et al., 2004; Epsztein et al., 2010; Chorev and Brecht, 2012; Coletta et al., 2018). The generation of these spikelets is voltage-dependent, where somatic hyperpolarization suppresses the spikelets and somatic depolarization promotes the spikelet incidence (Crochet et al., 2004; Chorev and Brecht, 2012). Moreover, these large-amplitude spikelets are sensitive to sodium channel blockers, which suggests that they are actively propagating within the recorded cells (Schmitz et al., 2001; Crochet et al., 2004). This spikelet type occurs as a single event or in bursts with short inter-spikelet intervals of few milliseconds (Figure 2B). Interestingly, the large-amplitude spikelets can trigger somatic APs, which show a distinct initial rising phase ('shoulder') that fits the spikelet waveform (Epsztein et al., 2010). In CA1 pyramidal neurons *in vivo*, firing rates of these spikelets show spatial modulation with place fields virtually identical to the place fields of somatic APs (Epsztein et al., 2010). In presubicular head-direction cells, spikelets and APs from a single cell exhibit virtually identical head-direction tuning (Coletta et al., 2018).

A different type of spikelet was also found in both neocortical (Figure 2C; Scholl et al., 2015) and hippocampal (Figure 2D; Valiante et al., 1995) pyramidal neurons. These spikelets exhibit smaller amplitudes (typically in the range of 1 mV) and a brief time course (width at

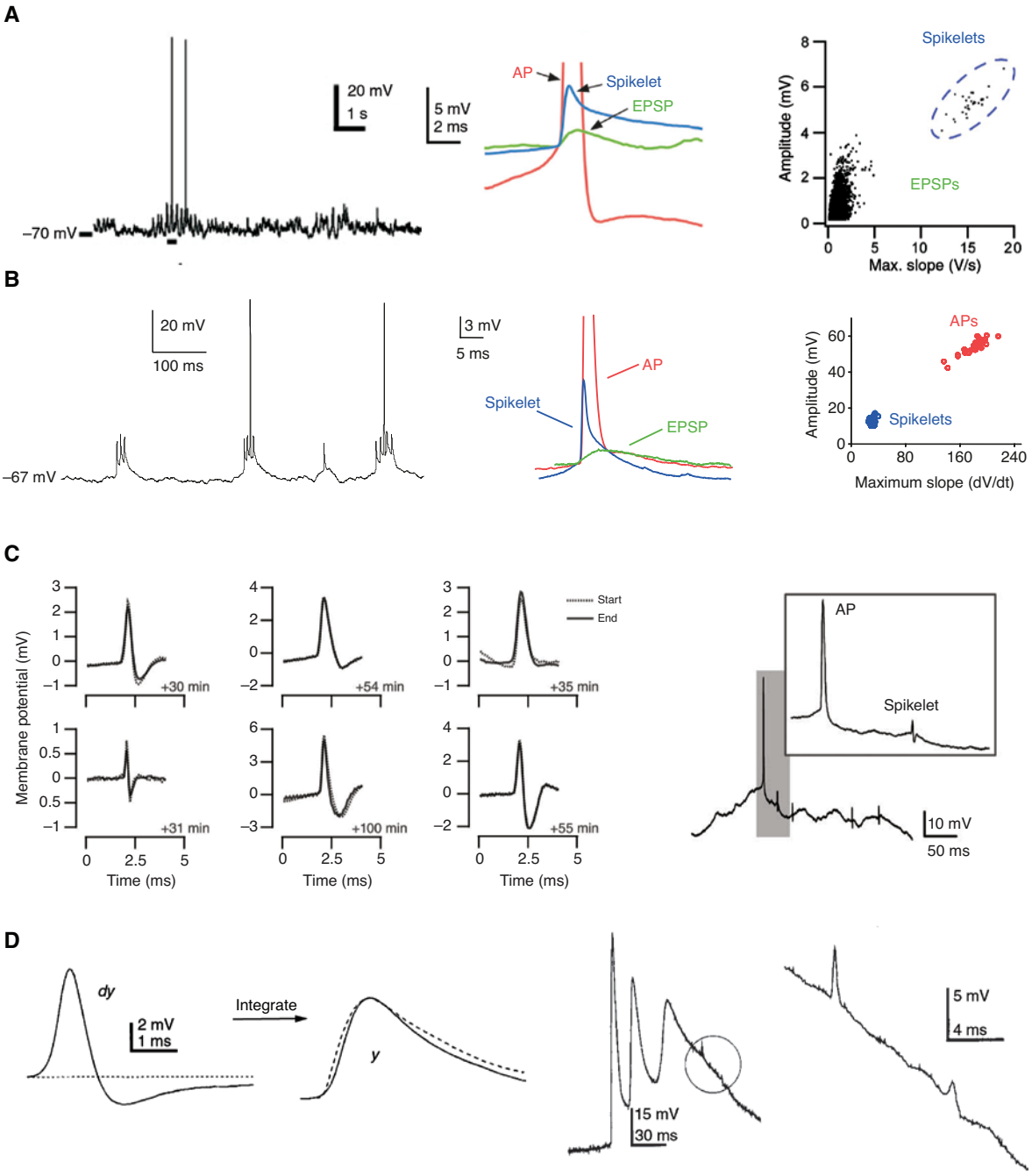

Figure 2: Two types of spikelets observed in pyramidal neurons.
(A, B) Large-amplitude spikelets recorded *in vivo* in putative pyramidal cells in cat neocortex (A; Crochet et al., 2004) and in hippocampal CA1 pyramidal neurons (B; Epsztein et al., 2010). Left: Example somatic voltage traces with APs and spikelets. Middle: Overlay of mean AP (red, truncated), spikelet (blue), and EPSP (green) waveforms. Right: The all-or-none nature of spikelets is revealed in plots of amplitude vs. maximum slope. (C, D) Spikelets with fast, often hyperpolarizing, decay. (C) Small-amplitude spikelets from neocortical principal cells recorded in cat visual cortex *in vivo* (Scholl et al., 2015). Left: Mean spikelet waveforms from individual cells, as recorded at the beginning (dotted line) and toward the end of the recording session (solid line). Time passed between the two averages is indicated for each example. Right: A voltage trace showing an AP and spikelets; the gray region is enlarged in the inset. Note that the spikelet waveform is briefer than the AP waveform. (D) Spikelets occurring in CA1 pyramidal neurons *in vitro* during calcium-free-induced epileptic activity (Valiante et al., 1995). Left: Average spikelet waveform from a single cell (d*y*). The spikelet corresponds to a differentiated AP: Numerically integrating the spikelet waveform (d*y*) results in a waveform (*y*) that qualitatively matches the averaged AP waveform recorded from another cell (dashed line). Right: AP burst with two spikelets encircled and expanded on the far right. (A) Reprinted from Crochet et al. (2004) by permission from Oxford University Press. (B) From Epsztein et al. (2010). Reprinted with permission from AAAS. (C) Reprinted from Scholl et al. (2015), with permission from John Wiley and Sons. (D) Republished with permission from Society for Neuroscience, from Valiante et al. (1995); permission conveyed through Copyright Clearance Center, Inc. (A–D) All rights reserved.

half-maximum amplitude <0.5 ms). Frequently, spikelets of several discrete amplitudes appear in a single cell, with inter-spikelet intervals similar to the inter-spike intervals. These small-amplitude spikelets occur independently of the somatic membrane potential or somatic APs. Accordingly, they are not suppressed by somatic hyperpolarization and were even observed superimposed on somatic AP bursts (Figure 2D). In CA1 pyramidal neurons, such spikelets were found during calcium-free-induced epileptic activity in slices (Valiante et al., 1995). Their occurrence correlated with population activity, as both were co-modulated by pH. Such brief spikelets were also reported in cat visual neocortex (Figure 2C; Scholl et al., 2015), where they shared several sensory selectivities with the APs, including orientation selectivity, receptive field location, and eye preference. However, binocular disparity tuning was typically not correlated between the APs and spikelets, and in half of the cells, the simple-cell/complex-cell receptive field properties did not match between APs and spikelets (Scholl et al., 2015).

The following sections review spikelet properties generated with the various mechanisms. We propose that the first type of spikelet (Figure 2A, B) fits best to axonal origin within a single cell; the second type of spikelet (Figure 2C, D) matches the properties of spikelets generated via ephaptic coupling to a neighboring cell.

Spikelets evoked by dendritic spikes

Historically, one of the first studies on spikelets in cortical neurons was carried out by Spencer and Kandel (1961). In 25% of units recorded in cat hippocampus *in vivo*, the authors observed fast events of small amplitudes (mean 5.9 ± 2.4 mV), which were initiated approximately 10 mV below the usual AP firing threshold of these cells. These events were called 'fast prepotentials' (FPPs), because they only occurred spontaneously in the rising phase of APs. To study the FPPs in isolation, hyperpolarizing pulses had to be delivered to the soma during spontaneous discharges (Figure 3A, B). A 'process of elimination' was applied to deduce the origin of these events: As FPPs were present in rebound responses to intracellularly delivered hyperpolarization (Figure 3B), the authors reasoned that they probably originated within the impaled neurons. The decay of isolated FPPs appeared faster than a purely passive process (Figure 3C), so active currents were postulated in FPP generation. Next, as the antidromically evoked APs never showed FPPs, the authors proposed that FPPs might reflect dendritic spikes that are attenuated on their way to the soma. Finally, the presence of FPPs in response to stimulation of fibers projecting to the apical dendrite let the authors conclude that the FPPs originated in the apical dendritic tree. Because of the

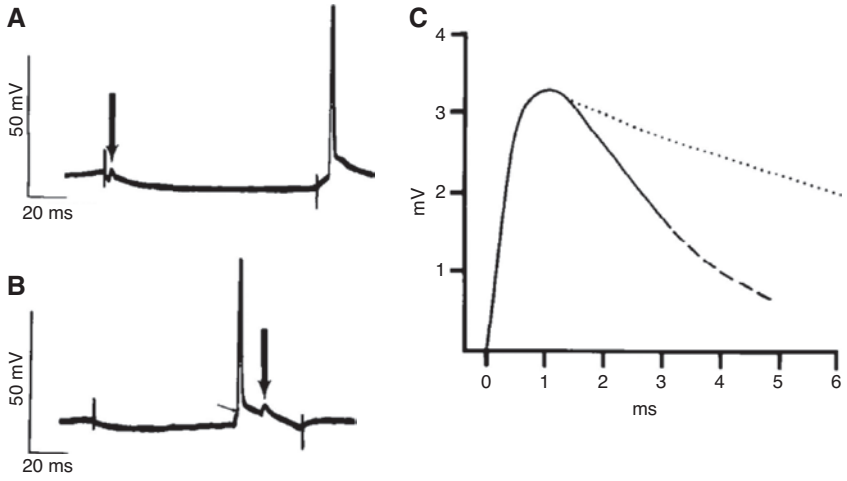

Figure 3: 'Fast prepotentials' (FPPs) in hippocampal pyramidal neurons *in vivo*.
(A) Weak somatic hyperpolarization (presumably applied between the two stimulation artifacts) can isolate FPPs (large vertical arrow, left) in somatic intracellular recordings. In this example, the rebound AP (right) does not show an FPP. (B) A rebound AP is preceded by an FPP (diagonal mark) and followed by an isolated FPP (large vertical arrow). (C) Waveform of an isolated FPP (solid line). The dashed part indicates 'the uncertainty in judging the baseline on which these small prepotentials ride'. Time course of a purely passive decay is depicted as a dotted line. Reprinted from Spencer and Kandel (1961) with permission from The American Physiological Society, all rights reserved.

stereotypic appearance and small amplitudes of FPPs, the underlying dendritic spikes were supposed to occur in a single discrete area of the dendritic tree, separated by passive membrane from the soma. Functionally, FPPs of apical dendritic origin would act as a 'booster' for 'otherwise ineffectual distal dendritic synapses' (Spencer and Kandel, 1961).

Subsequent studies in the following decades indeed found that several neuron types including neocortical and hippocampal pyramidal cells (Golding and Spruston, 1998) have active dendrites capable of producing fast sodium spikes. However, these dendritic spikes occur in a graded manner (Golding and Spruston, 1998), so they are unlikely to result in all-or-none spikelets such as those described by Spencer and Kandel (1961). Moreover, dendritic sodium channels undergo slow inactivation (Mickus et al., 1999), so they do not support high-frequency firing as is typical for spikelets *in vivo* (e.g. Wong and Stewart, 1992; Crochet et al., 2004; Epsztein et al., 2010). Dual somatic and dendritic intracellular recordings demonstrated that dendritic spikes evoked in the distal apical dendrites of pyramidal neurons often fail to propagate to the soma (Spruston, 2008). However, these failed spikes appear as wide depolarizations at the soma (Figure 4; Golding and Spruston, 1998). Jarsky et al. (2005) discovered that the propagation of distal apical dendritic spikes is substantially facilitated by the activation of more proximal synapses. They observed that some somatically subthreshold responses exhibited spikelets of dendritic origin, yet the amplitude variability of these spikelets was not reported. Interestingly, distal apical inputs in CA2 pyramidal cells were shown to efficiently trigger dendritic spikes, which propagated reliably to the soma (Sun et al., 2014). Somatic hyperpolarization or a local TTX application revealed large and fast spikelets (amplitudes of 30–40 mV and max. dV/dt of 40–50 V/s), however, with graded amplitudes (Sun et al., 2014).

Not only apical but also basal dendrites of pyramidal neurons contain active conductances and fire dendritic spikes. Here, the resulting somatic spikelets appear rather slow (max. dV/dt up to 10 V/s) and have a distinct shape: the initial sodium spikelet is followed by a slower NMDA-receptor-dependent depolarization (Losonczy et al., 2008; Figure 5A). The latter, however, can be blocked by recurrent inhibition (Müller et al., 2012; Figure 5B). Nonetheless, repetitive initiation of dendritic spikes as well as AP backpropagation was found to cause inactivation of sodium channels in basal dendrites lasting for hundreds of milliseconds, resulting in attenuated dendritic spikes (Remy et al., 2009). Together, these properties of dendritic spikes enable basal dendritic branches to function as 'independent processing units' (Remy et al., 2009), where local synchronous synaptic input can trigger dendritic spikes, which evoke precisely timed AP output.

Even though dendritic spikes are commonly assumed to underlie spikelets in pyramidal cells (Wong and Stewart, 1992; Crochet et al., 2004), the graded nature of dendritic spikes and the inability of dendrites to fire at higher frequencies do not fit to the all-or-none spikelets occurring at high frequencies in these studies. Similar to the reasoning

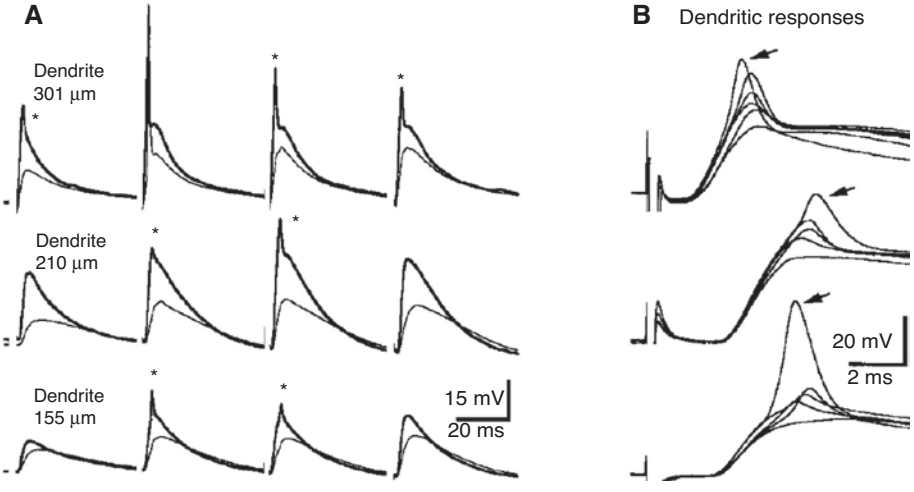

Figure 4: Propagation failures of apical dendritic spikes are not manifested as all-or-none somatic spikelets.
(A) Dual intracellular recordings in apical dendrites and the soma in three different CA1 pyramidal cells (rows). Shown are synaptically elicited dendritic spikes (asterisks, thick line) that failed to trigger a somatic AP (thin line: somatic traces). (B) Overlay of dendritic spikes from the three neurons shown in A reveal the graded nature of dendritic spikes. Arrows mark spikes that evoked somatic APs. Reprinted from Golding and Spruston (1998) with permission from Elsevier, all rights reserved.

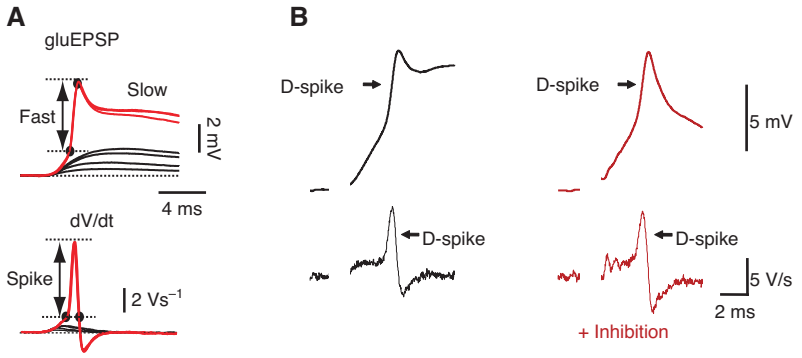

Figure 5: Spikelets originating in basal dendrites of CA1 pyramidal neurons.
(A) Subthreshold EPSPs (black) and dendritic spikes (red) evoked with uncaged glutamate, measured at the soma. Shown are voltage traces (top) and first time derivatives of voltage (bottom). The dendritic spikes exhibit two distinct components: an initial fast component and a late slow component. Reprinted by permission from Springer Nature Customer Service Centre GmbH: Nature, Losonczy et al. (2008). (B) Dendritic spikes evoked with glutamate iontophoresis in the absence (black) and in the presence (red) of recurrent inhibition, which blocks the slow spike component. Depicted are somatic voltage traces (top) and first time derivatives of voltage (bottom). Reprinted from Müller et al. (2012) with permission from Elsevier, all rights reserved.

of Spencer and Kandel (1961), the dendritic origin of spikelets is often concluded from the observation that spikelets can be evoked by dendritic but not somatic inputs. The study by Stuart et al. (1997) might help to resolve this paradox: the authors performed triple dendritic, somatic, and axonal recordings in layer V pyramidal neurons and demonstrated that output APs were always initiated in the axon before the soma, even when a dendritic spike preceded the somatic AP (Figure 6). This suggests that spikelets evoked by dendritic inputs do not necessarily reflect dendritic spikes, but might instead stem from axonal APs that are triggered by the dendritic spikes.

Spikelets generated by axonal APs

In this section, we propose that large-amplitude (3–30 mV) all-or-none spikelets occurring with short inter-spikelet intervals in the soma of pyramidal neurons (Crochet et al., 2004; Epsztein et al., 2010; Coletta et al., 2018) can originate from axonal APs, even when they are evoked with orthodromic (dendritic) stimuli. We first present insights from pioneering studies and complement them with the recent knowledge about the axon initial segment (AIS) where AP initiation occurs.

Axonal APs and spikelets have been studied in various neuron types as early as in the 1950s. Coombs et al. (1955) examined AP propagation in motoneurons and found that an axonal AP evoked with a distal axonal stimulus and propagating antidromically toward the soma might fail to activate a somatic AP and appear as an all-or-none spikelet when the somatic membrane voltage is hyperpolarized

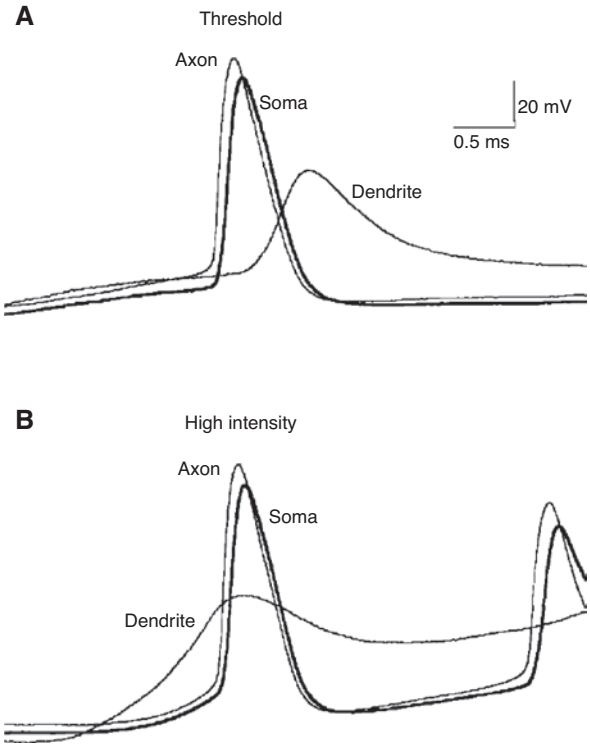

Figure 6: APs occur in the axon before the soma, even when a dendritic spike precedes the somatic AP.
Synaptic inputs were evoked with an extracellular electrode placed in layer 2/3, in the region of distal apical dendrites. Whole-cell patch-clamp recordings were obtained simultaneously at the soma (thick traces), apical dendrite (300 µm from soma), and axon (20 µm from soma). (A) A threshold-intensity stimulus resulted in AP initiation at the AIS, followed by a somatic AP and an attenuated backpropagating AP in the dendrite. (B) A strong stimulus elicited a dendritic spike first, but nevertheless, the axonal AP preceded the somatic AP. Reprinted from Stuart et al. (1997) with permission from John Wiley and Sons, all rights reserved.

(Figure 7A) or strongly depolarized (Figure 7B). The authors concluded that 'there is the same failure of invasion, both when the membrane is heavily depolarized and the activation mechanism is continuously partially engaged, and when the membrane is hyperpolarized and the axonal currents are insufficient to depolarize the membrane to the extent of setting off the activation mechanism' (Coombs et al., 1955). These observations hold also for pyramidal neurons, where somatic hyperpolarization is still a popular method to uncover and study antidromic axonal spikelets (Figure 7C; Hu et al., 2009).

Another way to generate antidromic spikelets is the so-called 'two-shock technique'. Here, pairs of brief stimuli are delivered to the distal axon, resulting in a pair of somatic APs. Then, the interstimulus interval is decreased until the failure of the second somatic AP occurs and the underlying (all-or-none) spikelet is unveiled (Figure 7D; Kandel et al., 1961). This effect can be explained by a shorter relative refractory period of the axon as compared to the soma (Chen et al., 2010) and fits to the common occurrence of spikelets in bursts with short inter-spikelet intervals (Wong and Stewart, 1992; Crochet et al., 2004; Epsztein et al., 2010; Coletta et al., 2018). Consequently, the antidromically evoked spikelet is shaped by axial currents generated during the axonal AP propagation that result in a relatively fast and strong somatic depolarization: the spikelet.

Thus, antidromic axonal spikelets can easily be triggered by distal axonal stimulation, but it is not clear whether they also occur spontaneously *in vivo*. Besides a subpopulation of cortical interneurons, where antidromic APs and antidromic spikelets are generated in response to naturally occurring input patterns (Sheffield et al., 2010), antidromic spikelets – also called 'ectopic' – are typically

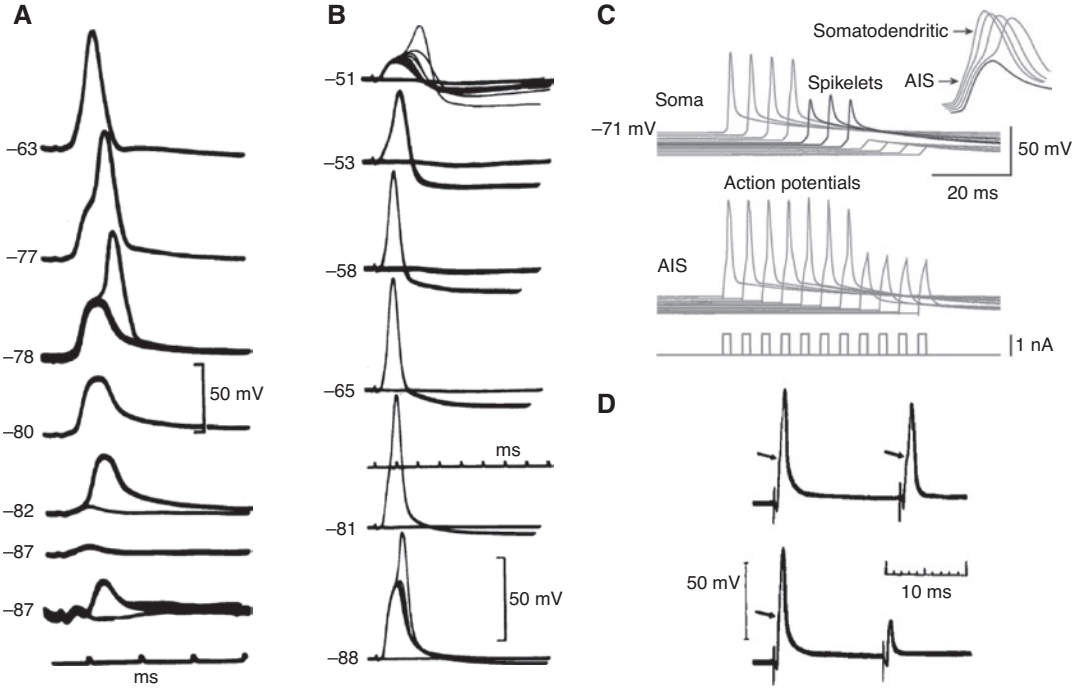

Figure 7: Antidromic generation of axonal spikelets.
(A) Somatic hyperpolarization of a motoneuron revealed all-or-none spikelets of axonal origin: a large spikelet (third to fifth rows) was postulated to result from AP propagation failure at the axon hillock-soma boundary. Further hyperpolarization uncovered a smaller spikelet (fifth and sixth rows; sixth row expanded 4.5× below), which was supposed to reflect an AP propagation failure at the transition from the myelinated to the non-myelinated axon. (B) Somatic depolarization of a motoneuron also resulted in all-or-none spikelets (first row), albeit the transition from full APs to spikelets appeared in a somewhat graded manner. (C) Somatic hyperpolarization disclosed spikelets in layer V pyramidal neurons (upper traces). The inset shows the correspondence between the initial rising phase of the APs ('shoulder', gray) and the rising phase of the spikelets (black). The simultaneous recordings from the AIS demonstrated APs corresponding to somatic spikelets (lower traces). (D) In a CA1 pyramidal neuron, applying a sequence of two brief stimuli to the axon results in two APs (first trace), but if the interstimulus interval is small enough, a spikelet is evoked with the second stimulus (second trace). The arrows mark the inflection in the rising phase of the APs corresponding to the spikelet. (A, B) Reprinted from Coombs et al. (1955) with permission from John Wiley and Sons. (C) Reprinted by permission from Springer Nature Customer Service Centre GmbH: Nature, Hu et al. (2009). (D) Reprinted from Kandel et al. (1961) with permission from The American Physiological Society.

reported in pyramidal neurons under various artificial or pathological conditions such as epilepsy (Avoli et al., 1998). These antidromic spikelets are characterized by an abrupt rise from the baseline without an underlying depolarization, and unlike orthodromic spikelets, they persist also during moderate somatic hyperpolarization. APs with these characteristics have been observed in *in vitro* models of gamma (Dugladze et al., 2012) and ripple oscillations (Bähner et al., 2011), but such ectopic APs were not found in recordings during ripple oscillations *in vivo* (English et al., 2014). However, antidromic spikelets would also result from axo-axonic coupling by gap junctions, which has been proposed for adult cortical pyramidal neurons (Schmitz et al., 2001; Hamzei-Sichani et al., 2007) and is reviewed in the section on electrotonic coupling.

For cortical pyramidal cells *in vivo*, inputs are usually considered to arrive at the soma orthodromically. It is not immediately evident how the mechanisms of antidromic spikelet generation might relate to orthodromic spikelets, i.e. spikelets evoked with dendritic synaptic inputs. Remarkably, Coombs et al. (1957) have shown in a series of experiments that 'when an impulse is generated in a motoneuron by synaptic or direct stimulation [of the soma], there is the same two-stage invasion [of the soma] as with antidromic activation, though the [temporal] interval between the small-spike [spikelet] and the large-spike is much less than with antidromic invasion […], and it is more difficult to block the impulse between the two stages'. In these experiments, Coombs et al. could evoke somatic spikelets with direct (orthodromic) stimulation using the effects of somatic hyperpolarization and refractoriness. For example, somatic spikelets could be triggered by a brief somatic depolarization immediately followed by a hyperpolarizing pulse (Figure 8). This closely resembles the situation described by Crochet et al. (2004): 'Cortical stimulation evoked a sequence of depolarization-hyperpolarizing potential; the early depolarization was crowned with an FPP [fast prepotential, i.e. a spikelet] when it reached the threshold for FPP generation'. The theoretical work by Michalikova et al. (2017) agrees with the above experimental results and demonstrates that the orthodromic inputs giving rise to spikelets are briefer and weaker than the inputs eliciting APs.

Interestingly, already Coombs et al. (1957) hypothesized that (orthodromic) somatic APs are initiated at the AIS where the firing threshold is about 10–20 mV lower than at the soma. This proposition was supported by early computational studies: Dodge and Cooley (1973) found that simulated motoneuron APs match the experimentally recorded waveforms when the AIS has a 10 mV lower

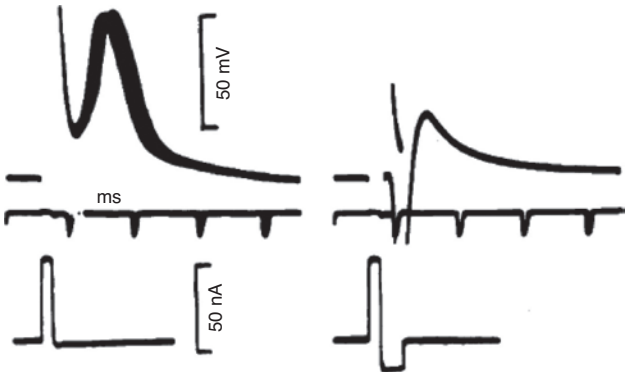

Figure 8: Orthodromic generation of spikelets.
APs evoked in a motoneuron with somatic current pulses (left). Orthodromic spikelets could be generated when a brief somatic depolarization was immediately followed by a hyperpolarizing pulse (right trace). The current input is depicted below the corresponding voltage trace. Reprinted from Coombs et al. (1957) with permission from John Wiley and Sons, all rights reserved.

threshold and 10 times larger sodium channel density than soma. Consequently, orthodromic spikelets might be viewed as (backpropagated) APs elicited at the AIS, which failed to trigger an AP at the soma. This failure does not happen as easily for orthodromic as for antidromic stimulation because the orthodromic stimulus depolarizes the soma closer to its threshold. However, the initial segment of vertebrate axons has been recently recognized as a distinct, complex, and plastic structure, involved in AP initiation and regulation of neuronal excitability. These recent findings support the possibility of axonal generation of spikelets and are reviewed in the information box 'AIS – the site of AP initiation'.

AIS – the site of AP initiation

The AIS has been implicated in the AP generation already decades ago (Coombs et al., 1957). Additionally, early anatomical research identified its distinct ultrastructure, characterized by microtubule bundles and a dense granular layer underneath the plasma membrane (Palay et al., 1968), which distinguishes the AIS from the rest of the axon. Yet only technical advances in the past decade enabled to study the unique molecular composition of the initial segment in great detail (Rasband, 2010), providing the basis for further electrophysiological experiments and modeling work.

Since the pioneering work by Coombs and others, many independent studies have confirmed the AIS as the usual site of AP initiation in various neuron types, including hippocampal (Meeks and Mennerick, 2007) and neocortical (Palmer and Stuart, 2006) pyramidal cells. Further studies suggested that the AP threshold is lowest in the AIS because of its high density of voltage-gated sodium channels, up to 50 times higher than at the soma (Kole and Stuart,

2008). However, subsequent studies revealed a little difference between the sodium channel density at the AIS and soma (Fleidervish et al., 2010) and that APs were found to be initiated in the AIS even when its sodium channel density falls below that of the soma (Lazarov et al., 2018). Converging lines of evidence indicated that APs in cortical pyramidal neurons are initiated in the distal part of the AIS (Palmer and Stuart, 2006), where a distinct subtype of Na_V channels was found to cluster (Royeck et al., 2008), activating at more hyperpolarized membrane potentials than somatic Na_V channels (Colbert and Pan, 2002). Finally, Hu et al. (2009) demonstrated in layer V pyramidal neurons that the low-threshold $Na_V1.6$ channels accumulate at the distal AIS and promote AP initiation. In contrast, the high-threshold $Na_V1.2$ channels aggregate at the proximal AIS and are responsible for the backpropagation of the AP to the soma (Figure 9). The shift of the activation and inactivation curves between proximal and distal axonal locations was found to lie between 7 (Colbert and Pan, 2002) and 13 mV (Hu et al., 2009), which has been postulated to reflect a difference between the $Na_V1.6$ and $Na_V1.2$ channel subtypes (Hu et al., 2009).

In addition to the shifted activation and inactivation curves, the two Na-channel subtypes $Na_V1.2$ and $Na_V1.6$ were shown to differ in several other properties as well (Rush et al., 2005). The axonal $Na_V1.6$ subunit was identified to generate larger persistent sodium current than the somatic $Na_V1.2$ subunit (Rush et al., 2005). The axonal persistent current was found to be active already at resting potentials and to contribute to the low firing threshold of the AIS and to the rapid AP initiation (Fleidervish et al., 2010). Relevant for spikelet generation is also the finding that the axonal $Na_V1.6$ subtype is able to better sustain high-frequency firing and conducts more current at high frequencies than the predominantly somatic $Na_V1.2$ channel subtype (Rush et al., 2005). This might, at least partly, be caused by the slow, cumulative inactivation that was found in somatodendritic but not in axonal sodium channels (Mickus et al., 1999), predicting that high-frequency axonal firing is accompanied by high-frequency occurrence of somatic spikelets, as has been observed, for example, by Crochet et al. (2004) or Epsztein et al. (2010).

Interestingly, a recent study investigating AP initiation in $Na_V1.6$-null pyramidal neurons demonstrated that the $Na_V1.6$ subtype is not necessary for the lower firing threshold at the AIS compared to the soma (Katz et al., 2018). Rather, the authors suggest that the hyperpolarizing shift in the activation of axonal sodium channels might be a result of molecular interactions within the AIS. The hyperpolarizing activation shift has also been shown to undergo activity-dependent plasticity, co-occurring with synaptic long-term potentiation and decreasing the threshold of AP initiation (Xu et al., 2005). As an alternative explanation for the AP initiation at the AIS, Baranauskas et al. (2013) highlighted the role of neuronal morphology. Their study demonstrated that the AP threshold is lowest at the distal end of the AIS beyond the clustered sodium channels, where the capacitive load from the soma is the lowest.

Besides the Na_V sodium channels, several potassium channel types are specifically localized in the axon and enriched at the AIS. The fast activating and slowly inactivating K_V1 channels are colocalized at high densities with $Na_V1.6$ subunits at the distal AIS but are rare at the soma. Kole et al. (2007) found that these potassium channels regulate the axonal AP waveform independently from the soma. Furthermore, the authors have shown that the AP width at the soma and the axon is modulated by different firing patterns: somatic APs become wider during high-frequency bursts, whereas axonal APs broaden during slow rhythmic activity (Kole et al., 2007). As the AP width at axon terminals controls the efficacy of excitatory synaptic transmission (Geiger and Jonas, 2000), this suggests that neuronal activity can be integrated in the axon independently from the soma.

The slowly activating and non-inactivating K_V7 channels are likewise abundant in the AIS. They generate the subthreshold M-current, which diminishes neuronal excitability by increasing the AP threshold. In CA1 pyramidal neurons, the M-current has been found to suppress the intrinsic spontaneous firing (Shah et al., 2008). Moreover, M-current inhibition via cholinergic receptor activation exerts homeostatic effects on neuronal excitability: whereas acute M-current inhibition increases neuronal excitability, sustained M-current inhibition gradually reduces the excitability through a distal shift of the AP initiation zone (Lezmy et al., 2017).

The studies reviewed above imply that the variety of ion channels specifically targeted to the AIS provide powerful possibilities to set and regulate neuronal excitability and AP generation. Indeed, recently emerging evidence indicates that the neuron type-specific differences in firing properties and AP waveform can be largely explained by differences in the composition and organization of the AISs (Lorincz and Nusser, 2008; Kress et al., 2010). Moreover, it has been shown that the AIS is a highly plastic region, and its length as well as position can undergo activity-dependent plasticity (Grubb and Burrone, 2010; Kuba et al., 2010; Lezmy et al., 2017).

The highly specialized structure of the AIS, which can be activated and regulated independently from the soma, can promote the generation of orthodromic spikelets. These spikelets originate at the AIS like regular APs but fail to elicit a somatic AP (Michalikova et al., 2017). Such spikelets are characterized by relatively fast (max. $dV/dt > 10$ V/s) and large (up to 20–30 mV) waveforms because of the large sodium currents evoked at the AIS. Unlike spikelets originating in dendritic spikes, axonal spikelets can occur at high frequencies because of the shorter refractory period of the axon in comparison to the soma. Finally, the generation of axonal (AIS) spikelets is dependent on the somatic membrane voltage due to the close proximity of the AIS.

Spikelets with these properties were reported in several *in vivo* studies (Figure 2A, B; Spencer and Kandel, 1961; Wong and Stewart, 1992; Crochet et al., 2004; Epsztein et al., 2010; Chorev and Brecht, 2012; Coletta et al., 2018), although only Coletta et al. (2018) implied an axonal origin of spikelets. It seems that the generation of spikelets upon dendritic inputs is an important factor misleading the interpretation. As discussed above and illustrated in Figure 6, the study by Stuart et al. (1997) directly demonstrated in neocortical pyramidal neurons that dendritic spikes can first initiate an AP at the AIS, which then triggers a somatic AP. Also recent studies in turtle pyramidal neurons (Larkum et al., 2008) and CA1 pyramidal neurons (Apostolides et al., 2016) suggest that spikelets triggered through dendritic stimulation might originate in axonal APs.

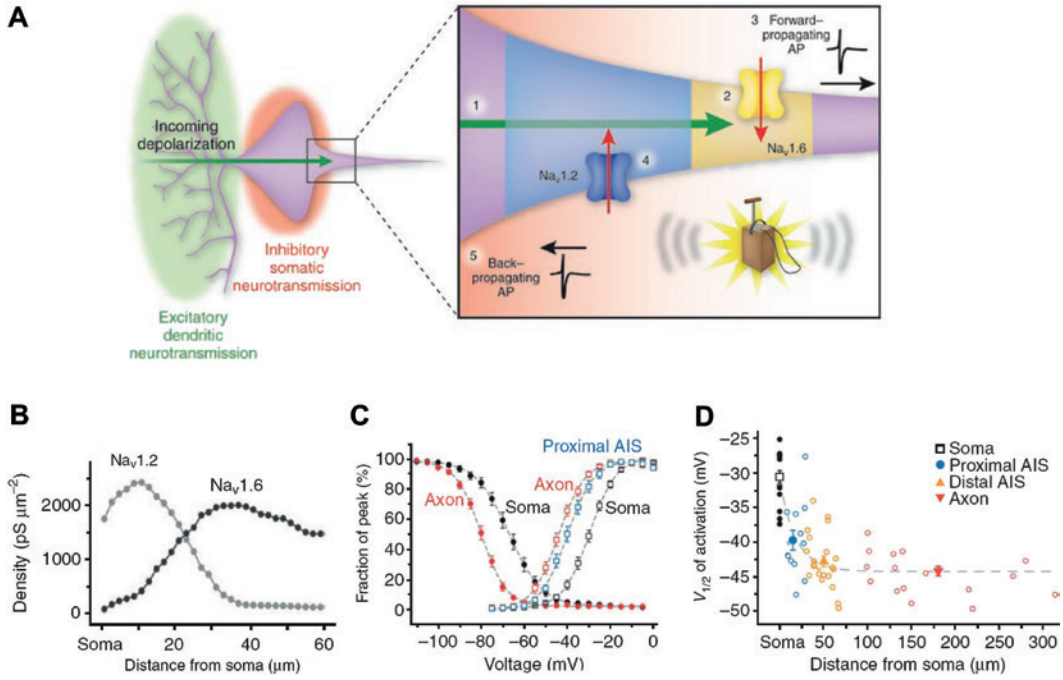

Figure 9: APs are initiated at the distal AIS.
(A) Schematic picture of AP initiation. Incoming depolarization (green arrow) initiates an AP in the distal AIS (yellow) where the low-threshold $Na_V1.6$ channels are localized. From there, the AP propagates forward along the axon as well as backpropagates to the soma. Reprinted by permission from Springer Nature Customer Service Centre GmbH: Nat Neurosci, Dulla and Huguenard (2009), all rights reserved. (B) Distribution of $Na_V1.2$ (gray) and $Na_V1.6$ (black) channel densities along the AIS, as estimated from immunofluorescence measurements. (C) Activation (empty squares) and inactivation (full circles) curves of somatic (black) and axonal (red) sodium currents. The activation curve for proximal AIS (blue) was added for comparison. (D) Half-activation voltages of sodium channels measured along the soma and axon. (B–D) Reprinted from Hu et al. (2009) with permission from Springer Nature; all rights reserved.

Orthodromically evoked spikelets of axonal origin have interesting functional consequences: the ability to generate output APs without firing an AP in the large somatodendritic compartments reduces the energetic costs of AP propagation (Ashida et al., 2007) and allows to control dendritic plasticity triggered by backpropagating APs (Spruston et al., 1995).

Spikelets resulting from electrotonic coupling by gap junctions

Another possibility for spikelet generation provides direct electrotonic coupling between pairs of neurons mediated via specialized structures called gap junctions. If two cells are coupled by such an electrical synapse, an AP occurring in one cell is transmitted through the gap junction and appears as a spikelet in the other cell.

Unlike chemical synapses, electrical synapses are reciprocal (though not necessarily symmetrical; Snipas et al., 2017), enabling passive current flow in both directions, depending on the potential gradient between the two connected compartments. The strength of electrotonic coupling, called *coupling coefficient*, is defined as the ratio of voltage change between the prejunctional and the postjunctional cell. The coupling coefficient depends on several factors: the junctional conductance, the transmitted voltage waveform (larger coupling coefficients for rectangular current injections than for AP waveforms), and the membrane properties of the postjunctional cell. The postjunctional membrane acts as a low-pass filter: the transmitted current first flows through the membrane capacitance, and as the capacitance gets charged, the current starts to flow through the membrane resistance. Consequently, slow fluctuations of the membrane potential are transmitted more effectively than fast signals like APs, which appear in the postjunctional cell as spikelets with slowed time courses and attenuated amplitudes (Figure 10A). Although the transmission of signals through gap junctions is immediate, an apparent delay can result from the time needed for capacitive loading of the postjunctional membrane to a detectable level (Bennett and Zukin, 2004).

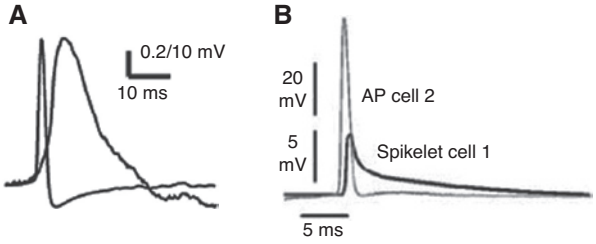

Figure 10: Spikelets in electrotonically coupled cells. (A) AP (briefer event) and the corresponding spikelet (wider event) recorded in a coupled pair of hippocampal stratum oriens interneurons. Amplitudes are scaled for a better comparison of their time course. Reprinted from Zhang et al. (2004) with permission from John Wiley and Sons, all rights reserved. (B) AP and the corresponding spikelet from a pair of CA1 pyramidal neurons. Amplitudes are scaled, but the short (<1 ms) time delay is as recorded experimentally. Reprinted from Mercer et al. (2006) with permission from Springer Nature; all rights reserved.

In the mammalian brain, gap junctions were first demonstrated by Sloper (1972) as dendrodendritic or dendrosomatic close membrane appositions with a dense, seven-layered structure. Later work has revealed that gap junctions consist of clusters of channels directly connecting the intracellular space of the two coupled neurons such that ions and small metabolites can pass through. Vertebrate gap junction channels are composed of proteins called *connexins*. In neurons, connexin 36 is the predominant gap-junctional protein (Connors and Long, 2004), although other connexins are present as well: for example, Cx45 was found in retinal neurons (Li et al., 2008), and Cx26 occurs in neonatal excitatory cells of the neocortex (Su et al., 2017).

In the adult brain, gap junctions have been thoroughly demonstrated to connect hippocampal and neocortical interneurons of the same type (reviewed, e.g., in Galarreta and Hestrin, 2001). First, dual recordings identified coupled pairs, where a subthreshold current injection or an AP in one cell resulted in a voltage change or a spikelet waveform, respectively, in the other cell. Next, anatomical studies delivered ultrastructural evidence for the existence of dendrodendritic or dendrosomatic gap junctions as early as in the 1970s (Sloper, 1972). Finally, molecular studies revealed that interneuron gap junctions are composed of connexin 36. The coupling between interneurons was found abundant, but rather weak, and the spikelet waveforms resulting from AP transmission through these electrical synapses exhibit small amplitudes (typically <1 mV) and slow dynamics (Figure 10A). These weak dendrodendritic and dendrosomatic gap junctions in cortical interneurons were shown to promote neuronal firing synchrony, thereby significantly contributing to the generation and maintenance of network oscillations, for example, the hippocampal gamma (Traub et al., 2001) and ripple oscillations (Holzbecher and Kempter, 2018).

In contrast, controversy still accompanies the notion of electrical coupling between adult cortical pyramidal cells. Here, the evidence is mostly composed of dye coupling data (based on gap junctional permeability for small tracer molecules such as neurobiotin, biocytin, or Lucifer yellow) and pharmacological modulation of spikelet occurrence and waveform. Up to date, only few studies demonstrated direct electrical coupling in pairs of adult hippocampal (MacVicar and Dudek, 1981; Mercer et al., 2006) and neocortical (Wang et al., 2010) pyramidal neurons, and one study provided anatomical evidence for the presence of gap junctions between mossy fiber axons in the dentate gyrus (Hamzei-Sichani et al., 2007). Moreover, the protein underlying the electrical coupling in pyramidal neurons remains unknown.

The spikelet waveforms found in dual recordings of pyramidal cells are substantially larger (2–20 mV) and faster than the waveforms typical of interneuron spikelets (Figure 10B) and resemble the spikelet waveforms recorded in pyramidal neurons *in vivo* (Figure 2A, B). Furthermore, unlike interneuron spikelets, spikelets in pyramidal neurons are abolished when the sodium channels of the recorded neuron are blocked intracellularly with QX314, which suggests that these spikelets propagate actively in the putative postjunctional neuron. Consistent with the fast spikelet waveform and active propagation in the recorded neuron is axo-axonal coupling, which has been suggested in some studies (Schmitz et al., 2001; Wang et al., 2010), but not in others (Mercer et al., 2006).

This evidence of gap junctional coupling in pyramidal neurons is weakened by inherent issues associated with the methods used to demonstrate gap junctional coupling. First, the paired recordings are typically performed with sharp electrodes as these allow successive penetration of many neurons before they get clogged and have to be exchanged (Bennett and Pereda, 2006). However, sharp electrodes are prone to the so-called 'shish-kebap artifact', where the recording electrode would penetrate more neurons at the same time and could introduce artifactual coupling. This problem also affects dye coupling experiments, where further artifacts might occur because of, for example, dye leakage into the extracellular space that can be taken up by adjacent neurons (Jefferys, 1995). However, some of the methodological challenges were overcome in recent studies (Schmitz et al., 2001; Mercer et al., 2006; see Bennett and Pereda, 2006, for review).

Up to now, there is one study providing direct ultrastructural evidence for gap junctions in cortical excitatory

neurons (Hamzei-Sichani et al., 2007). In thin-section transmission electron micrographs, the authors found altogether 10 close appositions of dentate granule axons called mossy fibers. Nonetheless, these putative gap junctions were missing the typical 'submembrane densities' and showed a pentalaminar instead of the typical heptalaminar structure. A further instance of a presumed axonal gap junction could be detected by freeze-fracture replica immunogold labeling using anti-Cx36 immunogold beads. However, it could not be determined whether the labeled axon was coupled to another axon or to a dendritic spine. Moreover, other studies did not find connexin 36 in pyramidal neurons (Hormuzdi et al., 2001; Pais et al., 2003).

Much more commonly, gap junctional coupling is inferred from modulatory effects of pH and pharmacology, although the effects of these manipulations are not specific to gap junctions (Connors and Long, 2004). For all connexins except Cx36, decreased intracellular pH (i.e. acidification) tends to close gap junctions, whereas increased intracellular pH (i.e. alkalization) opens gap junctions and strengthens electrical coupling (Connors and Long, 2004; González-Nieto et al., 2008). This behavior has been observed also for electrical coupling in pyramidal neurons (Schmitz et al., 2001). In contrast, gap junctions formed by Cx36 respond in an opposite manner, opening upon acidification and closing upon alkalization (González-Nieto et al., 2008). However, pH levels have been shown to regulate not only gap junctions but various membrane channels as well (Chesler, 2003). Moreover, the physiological regulation of neuronal pH appears to be homeostatic: neuronal activity leads to acidosis, which in turn diminishes the excitability of neurons. Elevated pH has the opposite effect of increasing neuronal excitability (Chesler, 2003).

There are various pharmacological agents shown to modulate the strength of electrotonic coupling. These are chemically diverse and include long-chain alcohols such as heptanol or octanol, the anesthetic halothane, carbenoxolone, and mefloquine. However, most of these substances act non-specifically and have been shown to influence other physiological properties of neurons as well (Connors and Long, 2004). The specificity of carbenoxolone is controversial, with some studies reporting no influence on intrinsic neuronal properties (Schmitz et al., 2001), while others found reduction of various membrane conductances, increased AP threshold, or decreased input resistance (Rouach et al., 2003; Tovar et al., 2009). The quinine derivate mefloquine has recently gained interest as a specific and potent blocker of Cx36 channels, but also here some side-effects have been reported (Cruikshank et al., 2004). Yet it needs to be considered that if pyramidal cells are coupled at axonal sites, the transmitted AP is propagated actively in the axon of the postjunctional cell, and the propagation failure occurs close to the soma. Therefore, the pharmacological modulation of spikelet amplitude unlikely reflects not only a modulation of axo-axonal gap junction itself but also a change of some other neuronal property.

To address the question whether electrotonic coupling occurs in pyramidal neurons *in vivo*, Chorev and Brecht (2012) performed dual intra- and extracellular recordings of CA1 pyramidal neurons in anesthetized rats. The authors identified an extracellular AP waveform associated with, and slightly preceding, the onset of intracellular spikelets. Simulations of extracellular waveforms of APs and spikelets in compartmental models of pyramidal neurons showed that electrotonic coupling can in theory account for all aspects of the data. It would require gap junctions between the axons, in combination with a large (>several 100 μm) distance between the somata of the coupled cells, such that only the intracellularly recorded cell shapes the extracellular waveform (Michalikova et al., 2018). In contrast, paired recordings in hippocampal (Mercer et al., 2006) and neocortical (Wang et al., 2010) pyramidal neurons demonstrated electrical and dye coupling in cells with somata located very close to each other (Figures 11 and 12), but the close membrane appositions found at proximal somatodendritic sites did not show any 'distinctive structures indicative of a gap junction' (Figure 11; Mercer et al., 2006).

In short, only few *in vitro* studies have shown directly, i.e. through dual recordings of coupled neurons, that spikelets in cortical pyramidal neurons can result from electrotonic coupling, and the anatomical evidence for gap junctions is scarce. Theoretical as well as some experimental studies have suggested an axonal coupling site, which could account for the relatively large amplitudes, fast time course, and active propagation of these spikelets in the postjunctional cell (Traub et al., 1999; Schmitz et al., 2001; Wang et al., 2010). Theoretical studies proposed that axo-axonal coupling of pyramidal neurons could underlie the generation of high-frequency oscillations such as hippocampal ripples (Traub et al., 1999), which is supported by experimental studies showing that *in vitro* ripples can occur without GABA-A receptors (Draguhn et al., 1998; Nimmrich et al., 2005). However, recent experimental studies indicate that also local inhibitory synaptic interactions can give rise to the ripple oscillation *in vitro* (Schlingloff et al., 2014) as

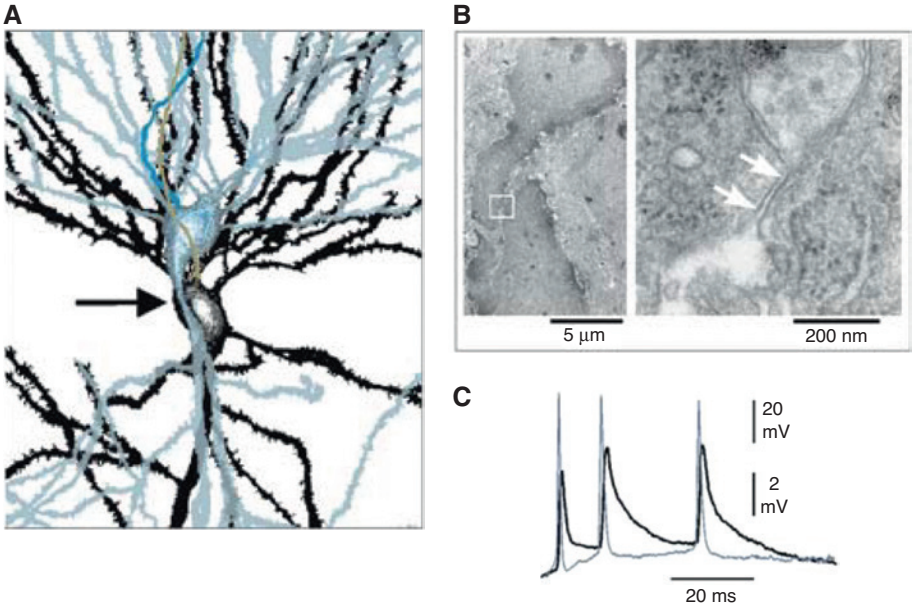

Figure 11: Electrical coupling in CA1 pyramidal neurons *in vitro*.
(A) Reconstruction of an electrically coupled pair of neurons. The arrow marks a putative contact between the apical dendrite of one cell (blue) and the soma of the other cell (black). (B) Left: Electron micrograph depicting the cells from (A) (proximal apical dendrite of the blue cell and both somata). The white box indicates the region of the putative contact site, which is expanded on the right. Note that the close membrane apposition, marked with white arrows, does not show any distinctive ultrastructure. (C) Demonstration of electrical coupling in the two cells shown in (A) and (B): APs in the blue cell (thin blue-gray traces) evoked spikelets in the black cells (black traces). Reprinted from Mercer et al. (2006) with permission from Springer Nature; all rights reserved.

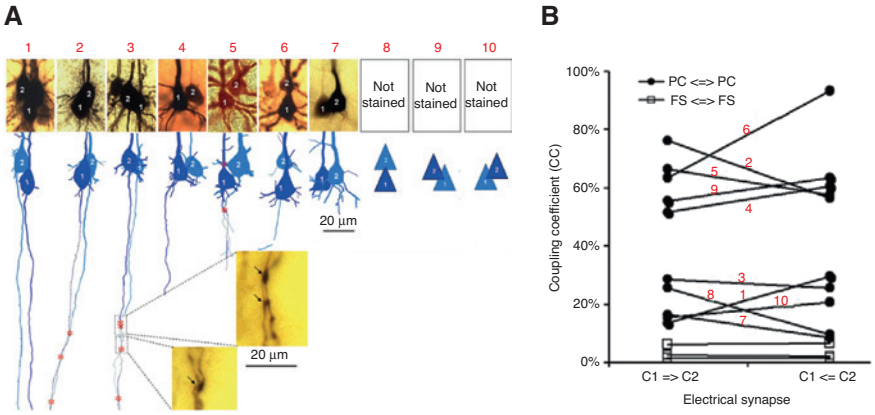

Figure 12: Electrical coupling in neocortical pyramidal neurons *in vitro*.
Morphologies (A) and coupling coefficients (B) of 10 coupled pairs of neocortical pyramidal neurons. In (A), red asterisks mark possible coupling sites, and insets show putative axo-axonal contacts. (B) Coupling coefficients (CCs) in both directions (cell 1 to cell 2, C1→C2, and cell 2 to cell 1, C2→C1) for all 10 pairs from (A). Three fast-spiking (FS) interneurons are included for comparison. The CCs were determined for step currents (nos. 2, 3, 6, and 10) or spikelet and AP transmission (nos. 1, 4, 5, and 7–9). Reprinted from Wang et al. (2010), used under the Creative Commons Attribution license. To view a copy of this license, visit https://creativecommons.org/licenses/by/4.0/.

well as *in vivo* (Stark et al., 2014). Spikelets generated by axo-axonal coupling are similar to spikelets evoked antidromically within a single neuron, as the AP transmitted through the gap junction propagates antidromically in the postjunctional axon and the spikelet emerges as a propagation failure at the soma. This similarity in mechanism, along with the inherent difficulty to prove gap-junction coupling, obscure the ultimate answer to the question whether gap junctions are present in adult pyramidal neurons.

Spikelets produced by ephaptic coupling

Ephaptic coupling is a form of electrical coupling between two cells without a specialized connection like a synapse or a gap junction. The term 'ephapse' (from Greek εφαπτω – to touch) was coined by Arvanitaki (1942) to describe 'the locus of contact or close vicinity of the active functional surfaces'. Such a close apposition of neuronal compartments enables transmission of electrical signals from one cell to another via extracellular electric fields. Here, we follow the seminal work by Jefferys (1995) and distinguish ephaptic coupling from population field effects. For the latter phenomenon, synchronized activity of many neurons generates large extracellular fields, which influence the membrane voltage of the entire neural population located within the reach of the field (Konnerth et al., 1984; Dudek et al., 1986). Indeed, the stereotypical spike-like waveforms of spikelets indicate that spikelets originate from individual APs. So when an AP is triggered in one cell, a spikelet waveform might be visible in another cell that has a process located in close proximity to the firing cell.

Unlike the 'resistive coupling' by gap junctions that results in slow, low-pass filtered spikelets, the nature of ephaptic AP transmission is capacitive: there is no transmembrane current flow, but the charge is redistributed on the intra- and extracellular surfaces of membranes (Valiante et al., 1995; Vigmond et al., 1997; Weiss and Faber, 2010). Consequently, the AP waveforms are high-pass filtered, and ephaptic spikelets appear brief, typically briefer than the underlying APs (Vigmond et al., 1997). The hallmark of ephaptic spikelets is a fast decay – on the same order as the rising phase – and a frequently observed biphasic shape (i.e. a depolarizing phase followed by a hyperpolarizing phase), which clearly distinguishes ephaptic spikelets from all other types of spikelets.

Such brief spikelets were observed in CA1 pyramidal neurons *in vitro* during calcium-free-induced epileptic activity where in every cell the amplitudes of spikelets occurred in two to four well-defined clusters (Valiante et al., 1995; Figure 2D). Another example of putative ephaptic spikelets is provided in the study by Scholl et al. (2015), which found that spikelets in cat visual cortex *in vivo* shared some, but not all, sensory selectivities with the APs recorded in the same cell (Figure 2C).

Amplitudes of these somatically recorded spikelets were several millivolt large (1–6 mV), which agrees with theoretical and modeling predictions for transmembrane voltage changes due to ephaptic AP transfer from a soma to a neuronal cable (Holt and Koch, 1999). However, Vigmond et al. (1997) noted that in a passive model of a CA3 pyramidal neuron, the amplitudes measured intracellularly were an order of magnitude smaller (<0.1 mV) than the induced transmembrane potentials. Holt and Koch (1999) pointed out that ephaptically generated transmembrane potentials do not spread electrotonically 'unless there are active channels at the location of the ephaptic depolarization'. Fast sodium currents active at subthreshold potentials could, in principle, boost the intracellular amplitudes of spikelets. Vigmond et al. (1997) alternatively proposed that intracellular spikelet amplitudes of several millivolts might be achieved by synchronized firing of several close-by neurons. This is conceivable for epileptic activity (Valiante et al., 1995) but rather unlikely to occur under physiological *in vivo* conditions (Scholl et al., 2015).

In general, ephaptic interactions are weak even for cells that are very close (3 nm apart in the model of Vigmond et al., 1997) because the AP waveform is transmitted through the low-resistance extracellular medium. Consistently, increased extracellular resistance has been shown to promote ephaptic coupling: Jefferys (1995) reviewed experiments with squid giant axons, where even APs could be evoked in an ephaptically coupled axon if the two nearby axons were immersed in mineral oil, which acts as an insulator and thus increases extracellular resistance. The physiological extracellular resistance is largest in brain regions with densely packed cells and restricted extracellular space like in rat hippocampus, especially in the CA1 cell body layer, which has double the resistivity of the surrounding layers (Gold et al., 2006). Moreover, the extracellular space is not constant over time but shrinks with intense neuronal activity that results in tissue swelling (Fox et al., 2004; Weiss and Faber, 2010). This might explain the occurrence of ephaptic spikelets in CA1 pyramidal neurons under epileptic conditions. However, neocortical tissue is less densely packed, and the *in vivo* activity is incomparable to epileptic states. So it is not immediately clear how ephaptic spikelets of several millivolts in amplitude can be generated in neocortical cells as observed by Scholl et al. (2015).

Cable theory posits that the voltage change induced by ephaptic coupling is smaller in thinner cables like axons than in thicker cables like dendrites (Holt and Koch, 1999). In contrast, Han et al. (2018) found ephaptic coupling between AISs of cerebellar Purkinje cells, which promotes firing synchrony in pairs of these cells. This coupling is enabled by the high density of sodium channel at the AIS,

Table 1: Overview of the spikelet-generating mechanisms.

Spikelet mechanism	All-or-none spikelets	Spikelet properties	Functional relevance in pyramidal neurons	Selected experimental and theoretical studies
Dendritic spikes, apical	No	1. Graded amplitudes 2. No spikelet bursts 3. In CA1 pyramidal neurons: Wide and slow depolarizations at the soma 4. In CA2 pyramidal neurons: Large (30–4 mV) and fast (dV/dt of 40–50 V/s) spikelets	Boosting of distal apical inputs	Experiment: Golding and Spruston (1998); Jarsky et al. (2005); Sun et al. (2014) Theory: Traub and Llinas (1977)
Dendritic spikes, basal	No	1. Graded amplitudes 2. No spikelet bursts 3. Slow spikelets (dV/dt < 10 V/s) 4. Spikelet can be followed by NMDA-depolarization plateau	Independent information processing at individual dendritic branches	Experiment: Losonczy et al. (2008); Remy et al. (2009); Müller et al. (2012) Theory: Traub and Llinas (1977)
Axonal APs, antidromic	Yes	1. Large (3–30 mV) and fast (max dV/dt 10–40 V/s) spikelets 2. Spikelets occur in bursts with short inter-spikelet intervals 3. Spikelets are abolished by intracellular sodium channel blockers 4. Spikelet decay is faster than purely passive decay 5. Spikelets arise abruptly from the baseline, without prior depolarization 6. Somatic threshold of spikelets is highly variable 7. Spikelets are not abolished by moderate somatic hyperpolarization	Indication of epileptic discharges	Experiment: Coombs et al. (1955); Avoli et al. (1998); Schmitz et al. (2001); Hu et al. (2009) Theory: Dodge and Cooley (1973); Michalikova et al. (2017)
Axonal APs, orthodromic	Yes	1. Large (3–30 mV) and fast (max dV/dt 10–40 V/s) spikelets 2. Spikelets occur in bursts with short inter-spikelet intervals 3. Spikelets are abolished by intracellular sodium channel blockers 4. Spikelet decay is faster than purely passive decay 5. Spikelets arise from a preceding (synaptic) depolarization 6. Somatic threshold of spikelets is depolarized w.r.t. resting membrane potential 7. Spikelets are abolished by somatic hyperpolarization	Energy saving; possibility to regulate dendritic plasticity caused by backpropagated APs	Experiment: Coombs et al. (1957); Crochet et al. (2004); Epsztein et al. (2010); Chorev and Brecht (2012); Coletta et al. (2018) Theory: Michalikova et al. (2017); Michalikova et al. (2018)

Table 1 (continued)

Spikelet mechanism	All-or-none spikelets	Spikelet properties	Functional relevance in pyramidal neurons	Selected experimental and theoretical studies
Gap junctions, somatodendritic	Yes	1. Amplitude and max dV/dt of spikelets depend on the strength of the gap junction coupling 2. Spikelets are low-pass filtered APs ('resistive coupling') 3. Spikelets are not abolished by intracellular sodium blockers	Firing synchrony that promotes generation and maintenance of network oscillations	Experiment: Mercer et al. (2006); Wang et al. (2010) Theory: Vigmond et al. (1997); Michalikova et al. (2017); Michalikova et al. (2018)
Gap junctions, axonal	Yes	1. Amplitude and max dV/dt of spikelets independent of the strength of the gap junction coupling 2. All properties of antidromic axonal spikelets apply here as well	Generation of hippocampal ripple oscillations	Experiment: Schmitz et al. (2001); Hamzei-Sichani et al. (2007); Wang et al. (2010) Theory: Traub et al. (1999); Michalikova et al. (2018)
Ephaptic coupling	Yes	1. Spikelets are high-pass filtered APs ('capacitive coupling') 2. Brief spikelets with fast decay 3. Spikelet amplitudes of 1–6 mV 4. Often biphasic spikelets: depolarization followed by hyperpolarization 5. Often several clusters of spikelets with different shape and amplitude within a single cell	Indication of *in vitro* epileptic activity (calcium-free); firing synchrony of neighboring neurons	Experiment: Valiante et al. (1995); Scholl et al. (2015) Theory: Jefferys (1995); Vigmond et al. (1997); Holt and Koch (1999); Weiss and Faber (2010)

such that the generated extracellular potentials are large enough to activate sodium channels in nearby axons.

Thus, further theoretical studies are needed to examine ephaptic coupling in active models and to identify factors that might result in relatively large spikelet amplitudes in the millivolt range. Future studies should also assess the effect of activity-dependent tissue swelling on ephaptic coupling and the occurrence of spikelets (Jefferys, 1995; Weiss and Faber, 2010). Finally, the potential functional role of ephaptically induced spikelets in pyramidal neurons needs to be understood. Similar to population field effects, ephaptic coupling can synchronize the firing of close-by neurons but without the influence on the whole network (Han et al., 2018). However, it is also possible that ephaptic spikelets in pyramidal neurons are an epiphenomenon – and, at best, an indicator – of the network state.

Conclusions

We have reviewed the various spikelet-generating mechanisms with the aim to understand the origin of spikelets in pyramidal neurons. Table 1 provides an overview of the different mechanisms including spikelet properties and functional implications of each of the mechanisms. We note that at least two qualitatively different all-or-none spikelets appear in the experimental literature. One spikelet type is defined by small amplitudes and a very brief time course (width at half-amplitude < 0.5 ms; Valiante et al., 1995; Scholl et al., 2015), which fits well to theoretical predictions of waveforms transmitted ephaptically through extracellular fields. More reports, however, are associated with the other spikelet type, which exhibits relatively large amplitudes (up to 30 mV) and fast rise times (max. dV/dt of 10–40 V/s; Crochet et al., 2004; Epsztein et al., 2010; Chorev and Brecht, 2012; Coletta et al., 2018). Several lines of evidence point to an axonal origin of these spikelets, especially the short inter-spikelet intervals, its large and fast waveform, its dependence on membrane polarization, and active conductance within the recorded neuron. Such axonal spikelets can be generated either in a single cell or in pairs of cells coupled with axonal gap junctions. Albeit the existence of axo-axonal gap junctions is controversial, more work is needed to definitely distinguish between these two mechanisms. The present review demonstrates that spikelets of different origin might occur within a single system and provides information that can help to elucidate the origin of spikelets also in other systems where this question is still not resolved.

Acknowledgments: This work was supported by the Deutsche Forschungsgemeinschaft (DFG, German Research Foundation: GRK1589/2; KE 788/3-1, Funder Id: http://dx.doi.org/10.13039/501100001659, SFB1315 – project number 327654276; the NeuroCure excellence cluster 2049; SPP 1665), the German Federal Ministry for Education (BMBF: Bernstein Center for Computational Neuroscience Berlin, Funder Id: http://dx.doi.org/10.13039/501100002347, Grant 01GQ1001A; Bernstein Focus Neuronal Foundations of Learning, Funder Id: http://dx.doi.org/10.13039/501100002347, Grant 01GQ0972; grants 01GQ1420B and 01GQ1403), the German-US-American Collaboration in Computational Neuroscience Episodic Memory (grant 01GQ1705), a BIH Delbrück Fellowship (Stiftung Charité), the Einstein Center for Neurosciences Berlin, and the IIPF grant of the Einstein Foundation Berlin. We would like to thank M. Brecht and E. Chorev for valuable discussions of the topic. Moreover, we would like to thank R. Traub for helpful discussions and feedback on the manuscript.

References

Apostolides, P.F., Milstein, A.D., Grienberger, C., Bittner, K.C., and Magee, J.C. (2016). Axonal filtering allows reliable output during dendritic plateau-driven complex spiking in CA1 neurons. Neuron *89*, 770–783.

Arvanitaki, A. (1942). Effects evoked in an axon by the activity of a contiguous one. J. Neurophysiol. *5*, 89–108.

Ashida, G., Abe, K., Funabiki, K., and Konishi, M. (2007). Passive soma facilitates submillisecond coincidence detection in the owl's auditory system. J. Neurophysiol. *97*, 2267–2282.

Avoli, M., Methot, M., and Kawasaki, H. (1998). GABA-dependent generation of ectopic action potentials in the rat hippocampus. Eur. J. Neurosci. *10*, 2714–2722.

Bähner, F., Weiss, E.K., Birke, G., Maier, N., Schmitz, D., Rudolph, U., Frotscher, M., Traub, R.D., Both, M., and Draguhn, A. (2011). Cellular correlate of assembly formation in oscillating hippocampal networks in vitro. Proc. Natl. Acad. Sci. USA *108*, E607–E616.

Baranauskas, G., David, Y., and Fleidervish, I.A. (2013). Spatial mismatch between the Na^+ flux and spike initiation in axon initial segment. Proc. Natl. Acad. Sci. USA *110*, 4051–4056.

Bennett, M. and Pereda, A. (2006). Pyramid power: principal cells of the hippocampus unite! Brain Cell. Biol. *35*, 5–11.

Bennett, M. and Zukin, R. (2004). Electrical coupling and neuronal synchronization in the mammalian brain. Neuron *41*, 495–511.

Chen, N., Yu, J., Qian, H., Ge, R., and Wang, J. (2010). Axons amplify somatic incomplete spikes into uniform amplitudes in mouse cortical pyramidal neurons. PLoS One *5*, e11868.

Chesler, M. (2003). Regulation and modulation of pH in the brain. Physiol. Rev. *83*, 1183.

Chorev, E. and Brecht, M. (2012). In vivo dual intra- and extracellular recordings suggest bi-directional coupling between CA1 pyramidal neurons. J. Neurophysiol. *108*, 1584–1593.

Colbert, C. and Pan, E. (2002). Ion channel properties underlying axonal action potential initiation in pyramidal neurons. Nat. Neurosci. *5*, 533–538.

Coletta, S., Zeraati, R., Nasr, K., Preston-Ferrer, P., and Burgalossi, A. (2018). Interspike interval analysis and spikelets in presubicular head-direction cells. J. Neurophysiol. *120*, 564–575.

Connors, B.W. and Kriegstein, A. (1986). Cellular physiology of the turtle visual cortex: distinctive properties of pyramidal and stellate neurons. J. Neurosci. *6*, 164–177.

Connors, B. and Long, M. (2004). Electrical synapses in the mammalian brain. Ann. Rev. Neurosci. *27*, 393–418.

Coombs, J., Eccles, J., and Fatt, P. (1955). The electrical properties of the motoneurone membrane. J. Physiol. *130*, 291–325.

Coombs, J., Curtis, D., and Eccles, J. (1957). The interpretation of spike potentials of motoneurones. J. Physiol. *139*, 198–231.

Crochet, S., Fuentealba, P., Timofeev, I., and Steriade, M. (2004). Selective amplification of neocortical neuronal output by fast prepotentials in vivo. Cereb. Cortex *14*, 1110–1121.

Cruikshank, S., Hopperstad, M., Younger, M., Connors, B., Spray, D., and Srinivas, M. (2004). Potent block of Cx36 and Cx50 gap junction channels by mefloquine. Proc. Natl. Acad. Sci. USA *101*, 12364–12369.

Dodge, F. and Cooley, J. (1973). Action potential of the motorneuron. IBM J. Res. Dev. *17*, 219–229.

Draguhn, A., Traub, R., Schmitz, D., and Jefferys, J. (1998). Electrical coupling underlies high-frequency oscillations in the hippocampus *in vitro*. Nature *394*, 189–192.

Dudek, F., Snow, R., and Taylor, C. (1986). Role of electrical interactions in synchronization of epileptiform bursts. Adv. Neurol. *44*, 593–617.

Dugladze, T., Schmitz, D., Whittington, M.A., Vida, I., and Gloveli, T. (2012). Segregation of axonal and somatic activity during fast network oscillations. Science *336*, 1458–1461.

Dulla, C. and Huguenard, J. (2009). Who let the spikes out? Nat. Neurosci. *12*, 959–960.

English, D.F., Peyrache, A., Stark, E., Roux, L., Vallentin, D., Long, M.A., and Buzsáki, G. (2014). Excitation and inhibition compete to control spiking during hippocampal ripples: intracellular study in behaving mice. J. Neurosci. *34*, 16509–16517.

Epsztein, J., Lee, A., Chorev, E., and Brecht, M. (2010). Impact of spikelets on hippocampal CA1 pyramidal cell activity during spatial exploration. Science *327*, 474–477.

Fleidervish, I., Lasser-Ross, N., Gutnick, M., and Ross, W. (2010). Na^+ imaging reveals little difference in action potential-evoked Na^+ influx between axon and soma. Nat. Neurosci. *13*, 852–860.

Fox, J.E., Bikson, M., and Jefferys, J.G. (2004). Tissue resistance changes and the profile of synchronized neuronal activity during ictal events in the low-calcium model of epilepsy. J. Neurophysiol. *92*, 181–188.

Fuentealba, P., Crochet, S., Timofeev, I., Bazhenov, M., Sejnowski, T., and Steriade, M. (2004). Experimental evidence and modeling studies support a synchronizing role for electrical coupling in the cat thalamic reticular neurons *in vivo*. Eur. J. Neurosci. *20*, 111–119.

Galarreta, M. and Hestrin, S. (2001). Electrical synapses between GABA-releasing interneurons. Nat. Rev. Neurosci. *2*, 425–433.

Geiger, J.R. and Jonas, P. (2000). Dynamic control of presynaptic Ca^{2+} inflow by fast-inactivating K^+ channels in hippocampal mossy fiber boutons. Neuron *28*, 927–939.

Gibson, J.R., Beierlein, M., and Connors, B.W. (2005). Functional properties of electrical synapses between inhibitory interneurons of neocortical layer 4. J. Neurophysiol. *93*, 467–480.

Gold, C., Henze, D., Koch, C., and Buzsaki, G. (2006). On the origin of the extracellular action potential waveform: a modeling study. J. Neurophysiol. *95*, 3113–3128.

Golding, N. and Spruston, N. (1998). Dendritic sodium spikes are variable triggers of axonal action potentials in hippocampal CA1 pyramidal neurons. Neuron *21*, 1189–1200.

González-Nieto, D., Gomez-Hernandez, J., Larrosa, B., Gutierrez, C., Munoz, M., Fasciani, I., O'Brien, J., Zappala, A., Cicirata, F., and Barrio, L. (2008). Regulation of neuronal connexin-36 channels by pH. Proc. Natl. Acad. Sci. USA *105*, 17169–17174.

Grubb, M. and Burrone, J. (2010). Activity-dependent relocation of the axon initial segment fine-tunes neuronal excitability. Nature *465*, 1070–1074.

Hamzei-Sichani, F., Kamasawa, N., Janssen, W., Yasumura, T., Davidson, K., Hof, P., Wearne, S., Stewart, M., Young, S., Rash, J.E., and Traub, R. (2007). Gap junctions on hippocampal mossy fiber axons demonstrated by thin-section electron microscopy and freeze–fracture replica immunogold labeling. Proc. Natl. Acad. Sci. USA *104*, 12548–12553.

Han, K.-S., Guo, C., Chen, C.H., Witter, L., Osorno, T., and Regehr, W.G. (2018). Ephaptic coupling promotes synchronous firing of cerebellar Purkinje cells. Neuron *100*, 564–578.

Holt, G. and Koch, C. (1999). Electrical interactions via the extracellular potential near cell bodies. J. Comp. Neurosci. *6*, 169–184.

Holzbecher, A. and Kempter, R. (2018). Interneuronal gap junctions increase synchrony and robustness of hippocampal ripple oscillations. Eur. J. Neurosci. *48*, 3446–3465.

Hormuzdi, S.G., Pais, I., LeBeau, F.E., Towers, S.K., Rozov, A., Buhl, E.H., Whittington, M.A., and Monyer, H. (2001). Impaired electrical signaling disrupts gamma frequency oscillations in connexin 36-deficient mice. Neuron *31*, 487–495.

Hu, W., Tian, C., Li, T., Yang, M., Hou, H., and Shu, Y. (2009). Distinct contributions of $Na_V1.6$ and $Na_V1.2$ in action potential initiation and backpropagation. Nat. Neurosci. *12*, 996–1002.

Hughes, S., Blethyn, K., Cope, D., and Crunelli, V. (2002). Properties and origin of spikelets in thalamocortical neurones *in vitro*. Neurosci. *110*, 395–401.

Jarsky, T., Roxin, A., Kath, W.L., and Spruston, N. (2005). Conditional dendritic spike propagation following distal synaptic activation of hippocampal CA1 pyramidal neurons. Nat. Neurosci. *8*, 1667–1676.

Jefferys, J. (1995). Nonsynaptic modulation of neuronal activity in the brain: electric currents and extracellular ions. Physiol. Rev. *75*, 689–723.

Kandel, E., Spencer, W., and Brinley, F. (1961). Electrophysiology of hippocampal neurons: I. Sequential invasion and synaptic organization. J. Neurophysiol. *24*, 225–242.

Kaplan, E. and Shapley, R. (1984). The origin of the S (slow) potential in the mammalian lateral geniculate nucleus. Exp. Brain. Res. *55*, 111–116.

Katz, E., Stoler, O., Scheller, A., Khrapunsky, Y., Goebbels, S., Kirchhoff, F., Gutnick, M.J., Wolf, F., and Fleidervish, I.A. (2018). Role of sodium channel subtype in action potential generation by neocortical pyramidal neurons. Proc. Natl. Acad. Sci. USA *115*, E7184–E7192.

Kole, M. and Stuart, G. (2008). Is action potential threshold lowest in the axon? Nat. Neurosci. *11*, 1253–1255.

Kole, M., Letzkus, J., and Stuart, G. (2007). Axon initial segment Kv1 channels control axonal action potential waveform and synaptic efficacy. Neuron *55*, 633–647.

Konnerth, A., Heinemann, U., and Yaari, Y. (1984). Slow transmission of neural activity in hippocampal area CA1 in absence of active chemical synapses. Nature *307*, 69–71.

Kress, G., Dowling, M., Eisenman, L., and Mennerick, S. (2010). Axonal sodium channel distribution shapes the depolarized action potential threshold of dentate granule neurons. Hippocampus *20*, 558–571.

Kuba, H., Oichi, Y., and Ohmori, H. (2010). Presynaptic activity regulates Na^+ channel distribution at the axon initial segment. Nature *465*, 1075–1078.

Larkum, M.E., Watanabe, S., Lasser-Ross, N., Rhodes, P., and Ross, W.N. (2008). Dendritic properties of turtle pyramidal neurons. J. Neurophysiol. *99*, 683–694.

Lazarov, E., Dannemeyer, M., Feulner, B., Enderlein, J., Gutnick, M.J., Wolf, F., and Neef, A. (2018). An axon initial segment is required for temporal precision in action potential encoding by neuronal populations. Sci. Adv. *4*, eaau8621.

Lezmy, J., Lipinsky, M., Khrapunsky, Y., Patrich, E., Shalom, L., Peretz, A., Fleidervish, I.A., and Attali, B. (2017). M-current inhibition rapidly induces a unique CK2-dependent plasticity of the axon initial segment. Proc. Natl. Acad. Sci. USA *114*, E10234–E10243.

Li, X., Kamasawa, N., Ciolofan, C., Olson, C.O., Lu, S., Davidson, K.G., Yasumura, T., Shigemoto, R., Rash, J.E., and Nagy, J.I. (2008). Connexin45-containing neuronal gap junctions in rodent retina also contain connexin36 in both apposing hemiplaques, forming bihomotypic gap junctions, with scaffolding contributed by zonula occludens-1. J. Neurosci. *28*, 9769–9789.

Llinas, R., Baker, R., and Sotelo, C. (1974). Electrotonic coupling between neurons in cat inferior olive. J. Neurophysiol. *37*, 560–571.

Lorincz, A. and Nusser, Z. (2008). Cell-type-dependent molecular composition of the axon initial segment. J. Neurosci. *28*, 14329–14340.

Losonczy, A., Makara, J.K., and Magee, J.C. (2008). Compartmentalized dendritic plasticity and input feature storage in neurons. Nature *452*, 436–441.

MacVicar, B.A. and Dudek, F.E. (1981). Electrotonic coupling between pyramidal cells: a direct demonstration in rat hippocampal slices. Science *213*, 782–785.

Meeks, J. and Mennerick, S. (2007). Action potential initiation and propagation in CA3 pyramidal axons. J. Neurophysiol. *97*, 3460–3472.

Mercer, A., Bannister, A., and Thomson, A. (2006). Electrical coupling between pyramidal cells in adult cortical regions. Brain Cell. Biol. *35*, 13–27.

Michalikova, M., Remme, M.W.H., and Kempter, R. (2017). Spikelets in pyramidal neurons: action potentials initiated in the axon initial segment that do not activate the soma. PLoS Comp. Biol. *13*, e1005237.

Michalikova, M., Remme, M.W.H., and Kempter, R. (2018). Extracellular waveforms reveal an axonal origin of spikelets in pyramidal neurons. J. Neurophysiol. *120*, 1484–1495.

Mickus, T., Jung, H.-y., and Spruston, N. (1999). Properties of slow, cumulative sodium channel inactivation in rat hippocampal CA1 pyramidal neurons. Biophys. J. *76*, 846–860.

Müller, C., Beck, H., Coulter, D., and Remy, S. (2012). Inhibitory control of linear and supralinear dendritic excitation in CA1 pyramidal neurons. Neuron *75*, 851–864.

Nimmrich, V., Maier, N., Schmitz, D., and Draguhn, A. (2005). Induced sharp wave-ripple complexes in the absence of synaptic inhibition in mouse hippocampal slices. J. Physiol. *563*, 663–670.

Pais, I., Hormuzdi, S.G., Monyer, H., Traub, R.D., Wood, I.C., Buhl, E.H., Whittington, M.A., and LeBeau, F.E. (2003). Sharp wave-like activity in the hippocampus in vitro in mice lacking the gap junction protein connexin 36. J. Neurophysiol. *89*, 2046–2054.

Palay, S., Sotelo, C., Peters, A., and Orkand, P. (1968). The axon hillock and the initial segment. J. Cell. Biol. *38*, 193–201.

Palmer, L. and Stuart, G. (2006). Site of action potential initiation in layer 5 pyramidal neurons. J. Neurosci. *26*, 1854–1863.

Rasband, M. (2010). The axon initial segment and the maintenance of neuronal polarity. Nat. Rev. Neurosci. *11*, 552–562.

Remy, S., Csicsvari, J., and Beck, H. (2009). Activity-dependent control of neuronal output by local and global dendritic spike attenuation. Neuron *61*, 906–916.

Rouach, N., Segal, M., Koulakoff, A., Giaume, C., and Avignone, E. (2003). Carbenoxolone blockade of neuronal network activity in culture is not mediated by an action on gap junctions. J. Physiol. *553*, 729–745.

Royeck, M., Horstmann, M., Remy, S., Reitze, M., Yaari, Y., and Beck, H. (2008). Role of axonal $Na_v1.6$ sodium channels in action potential initiation of CA1 pyramidal neurons. J. Neurophysiol. *100*, 2361–2380.

Rush, A., Dib-Hajj, S., and Waxman, S. (2005). Electrophysiological properties of two axonal sodium channels, $Na_v1.2$ and $Na_v1.6$, expressed in mouse spinal sensory neurones. J. Physiol. *564*, 803–815.

Schlingloff, D., Káli, S., Freund, T.F., Hájos, N., and Gulyás, A.I. (2014). Mechanisms of sharp wave initiation and ripple generation. J. Neurosci. *34*, 11385–11398.

Schmitz, D., Schuchmann, S., Fisahn, A., Draguhn, A., Buhl, E., Petrasch-Parwez, E., Dermietzel, R., Heinemann, U., and Traub, R. (2001). Axo-axonal coupling: a novel mechanism for ultrafast neuronal communication. Neuron *31*, 831–840.

Scholl, B., Andoni, S., and Priebe, N.J. (2015). Functional characterization of spikelet activity in the primary visual cortex. J. Physiol. *593*, 4979–4994.

Shah, M., Migliore, M., Valencia, I., Cooper, E., and Brown, D. (2008). Functional significance of axonal K_v7 channels in hippocampal pyramidal neurons. Proc. Natl. Acad. Sci. USA *105*, 7869–7874.

Sheffield, M., Best, T., Mensh, B., Kath, W., and Spruston, N. (2010). Slow integration leads to persistent action potential firing in distal axons of coupled interneurons. Nat. Neurosci. *14*, 200–207.

Sloper, J. (1972). Gap junctions between dendrites in the primate neocortex. Brain. Res. *44*, 641–646.

Snipas, M., Rimkute, L., Kraujalis, T., Maciunas, K., and Bukauskas, F.F. (2017). Functional asymmetry and plasticity of electrical synapses interconnecting neurons through a 36-state model of gap junction channel gating. PLoS Comp. Biol. *13*, e1005464.

Spencer, W. and Kandel, E. (1961). Electrophysiology of hippocampal neurons: IV. Fast prepotentials. J. Neurophysiol. *24*, 272–285.

Spruston, N. (2008). Pyramidal neurons: dendritic structure and synaptic integration. Nat. Rev. Neurosci. *9*, 206–221.

Spruston, N., Schiller, Y., Stuart, G., and Sakmann, B. (1995). Activity-dependent action potential invasion and calcium influx into hippocampal CA1 dendrites. Science *268*, 297–300.

Stark, E., Roux, L., Eichler, R., Senzai, Y., Royer, S., and Buzsáki, G. (2014). Pyramidal cell-interneuron interactions underlie hippocampal ripple oscillations. Neuron *83*, 467–480.

Stuart, G., Schiller, J., and Sakmann, B. (1997). Action potential initiation and propagation in rat neocortical pyramidal neurons. J. Physiol. *505*, 617–632.

Su, X., Chen, J.-J., Liu, L.-Y., Huang, Q., Zhang, L.-Z., Li, X.-Y., He, X.-N., Lu, W., Sun, S., Li, H., et al. (2017). Neonatal CX26 removal impairs neocortical development and leads to elevated anxiety. Proc. Natl. Acad. Sci. USA *114*, 3228–3233.

Sun, Q., Srinivas, K.V., Sotayo, A., and Siegelbaum, S.A. (2014). Dendritic Na^+ spikes enable cortical input to drive action potential output from hippocampal CA2 pyramidal neurons. eLife *3*, e04551.

Tovar, K., Maher, B., and Westbrook, G. (2009). Direct actions of carbenoxolone on synaptic transmission and neuronal membrane properties. J. Neurophysiol. *102*, 974–978.

Traub, R., Schmitz, D., Jefferys, J., and Draguhn, A. (1999). High-frequency population oscillations are predicted to occur in hippocampal pyramidal neuronal networks interconnected by axo-axonal gap junctions. Neurosci. *92*, 407–426.

Traub, R.D., Kopell, N., Bibbig, A., Buhl, E.H., LeBeau, F.E., and Whittington, M.A. (2001). Gap junctions between interneuron dendrites can enhance synchrony of gamma oscillations in distributed networks. J. Neurosci. *21*, 9478–9486.

Valiante, T., Perez Velazquez, J., Jahromi, S., and Carlen, P. (1995). Coupling potentials in CA1 neurons during calcium-free-induced field burst activity. J. Neurosci. *15*, 6946–6956.

Vigmond, E., Perez Velazquez, J., Valiante, T., Bardakjian, B., and Carlen, P. (1997). Mechanisms of electrical coupling between pyramidal cells. J. Neurophysiol. *78*, 3107–3116.

Wang, Y., Barakat, A., and Zhou, H. (2010). Electrotonic coupling between pyramidal neurons in the neocortex. PLoS One *5*, e10253.

Weiss, S.A. and Faber, D.S. (2010). Field effects in the CNS play functional roles. Front. Neural. Circuit. *4*, 15.

Wong, R. and Stewart, M. (1992). Different firing patterns generated in dendrites and somata of CA1 pyramidal neurones in guinea-pig hippocampus. J. Physiol. *457*, 675–687.

Xu, J., Kang, N., Jiang, L., Nedergaard, M., and Kang, J. (2005). Activity-dependent long-term potentiation of intrinsic excitability in hippocampal CA1 pyramidal neurons. J. Neurosci. *25*, 1750–1760.

Zhang, Y., Perez Velazquez, J., Tian, G., Wu, C., Skinner, F., Carlen, P., and Zhang, L. (1998). Slow oscillations (≤ 1 Hz) mediated by GABAergic interneuronal networks in rat hippocampus. J. Neurosci. *18*, 9256–9268.

Zhang, X., Zhang, L., and Carlen, P. (2004). Electrotonic coupling between stratum oriens interneurons in the intact in vitro mouse juvenile hippocampus. J. Physiol. *558*, 825–839.